minerals

MDPI

Article

Geochemistry and Geochronology of the Huangcha Pluton and Tectonic Significance

Shuping Cao [1], Lun Li [2], Chonghui Yang [3] and Yongqiang Yang [1,*]

[1] State Key Laboratory of Geological and Mineral Resources, China University of Geosciences, Beijing 100083, China; dxyq8@cugb.edu.cn
[2] Beijing Jingneng Geological Engineering Co., Ltd., Beijing 102300, China; cugblilun@163.com
[3] Institute of Geology, China Academy of Geological Sciences, Beijing 100037, China; chhyang@cags.ac.cn
* Correspondence: yangyonq@cugb.edu.cn

Abstract: The Zanhuang Complex is situated on the eastern margin of the Trans-North China Orogen, with the Huangcha Pluton being a constituent of this complex. To ascertain the nature of the approximately 2.5-billion-year-old Huangcha Pluton, crucial evidence for understanding its extensional setting was sought through petrogenesis and dating investigations. LA-ICP-MS dating of zircon from the granite yielded an age of (2488 ± 6) Ma. Primarily composed of porphyritic monzonite with sporadic melanocratic enclaves, the Pluton's phenocrysts are predominantly feldspar with minor quartz. The granite exhibits high SiO_2 content (72.64%–74.16%) and alkali levels, with $Na_2O + K_2O$ ranging from 7.59% to 9.07%, classifying it as a shoshonitic series with a slightly peraluminous feature. Enrichment in large-ion lithophile (LIL) elements (Rb, Th, and U) and depletion in Sr, V, Cr, Co, and Ni were observed, with high Rb/Sr and Ga/Al ratios ranging from 0.73 to 2.72 and 2.75×10^{-4} to 3.11×10^{-4}, respectively. The rock exhibits high εNd(t) values, ranging from −0.06 to 0.88, with TDM2 ages falling between 2.79 and 2.87 billion years. Zircon grains display $^{176}Hf/^{177}Hf$ ratios ranging from 0.281266 to 0.281412 and εHf(t) values spanning from 0.96 to 6.18, calculated using the $^{207}Pb/^{206}Pb$ age. It is suggested that the Huangcha Pluton represents A-type granite formed via anatexis of the Neoarchean TTG in an extensional setting following orogenic processes. The formation of the Huangcha Pluton further corroborates the stabilization of the North China Craton towards the end of the Neoarchean. This finding supports the hypothesis that the North China Craton may belong to the Rae-family cratons, sharing similar magmatic and tectono-metamorphic records around ~2.5 billion years ago.

Keywords: geochemistry; the Huangcha Pluton; Neoarchean; tectonic setting; North China Craton

Citation: Cao, S.; Li, L.; Yang, C.; Yang, Y. Geochemistry and Geochronology of the Huangcha Pluton and Tectonic Significance. *Minerals* **2024**, *14*, 520. https://doi.org/10.3390/min14050520

Academic Editors: Simon Paul Johnson, Zhuang Li, Zhanzhan Duan, Ting Liu and Hafiz U. Rehman

Received: 20 April 2024
Revised: 11 May 2024
Accepted: 13 May 2024
Published: 17 May 2024

1. Introduction

The Neoarchean (2.8–2.5 Ga) is a crucial period marked by significant changes in the Earth's behavior, potentially representing the initial stage following a substantial growth of continental crust and formation of a habitable surface condition [1–4]. The Archean supracrustal belt provides a unique window into the tectonic evolution of the continental crust during this period. The volcano-sedimentary rocks and granitoid rocks in the late Neoarchean granite greenstone belts (GGBs) display a formation age of 2.60–2.48 Ga and metamorphic age of 2.52–2.47 Ga in the Zanhuang Complex of the Trans-North China Orogen, North China Craton [5].

It is widely accepted that A-type granites form within extensional tectonic settings, signifying the conclusion of orogenic activity [6]. The timing of the North China Craton's amalgamation remains contentious. Several viewpoints exist: some propose that during the late Archean, the western North China plate began subducting eastwards, with the two plates converging near the middle tectonic belt around 1.85 billion years ago [7–9]. Others suggest that the eastern plate subducted westwards, leading to craton assembly at the end of the Archean [10–14]. A two-staged island-arc accretion model posits that the east and west plates coalesced around 2.1 billion years ago [15,16]. Additional models with variations in cratonization timing exist, warranting further investigation. Intensive tectono-magmatic events nearly 2.5 billion years ago are well-documented in the North China Craton [17–19]. However, reports of A-type granite dating to ~2.5 billion years ago in the Zanhuang area are scarce. To date, Yang et al. [20] is the only group to report the Jiandeng A-type granite in the Zanhuang area, dated to 2506 ± 13 million years ago. Hence, the identification of A-type granite in the Zanhuang area formed within an extensional tectonic setting holds significant implications for understanding the timing of craton amalgamation events in the North China Craton.

Accurate geochronological boundaries are crucial for geological research, facilitating successful regional surveys and ore deposit prospecting. Currently, the age of the Guandu group lacks precise chronological constraints. Previously, it was regarded as part of the Zanhuang group. However, recent regional geological surveys in the Ningcheng area at a scale of 1:50,000 revealed that the Guandu group unconformably overlays Neoarchean gneiss. Rb-Sr whole-rock dating of magnetite-bearing muscovite quartz schist from the Guandu group yielded an age of 2061.42 ± 148 million years, interpreted as a metamorphic age. Furthermore, zircon U-Pb dating yielded a concordia age of 2210 million years for the Huangcha Pluton, which intruded the Guandu group. Consequently, the age of the Guandu group is inferred to be early Proterozoic. However, Wang et al. [21] contested this conclusion, citing the large error margin in the Pluton's dating, which they argue does not accurately reflect the Guandu group's formation age. Instead, based on correlations between the Paleo-Proterozoic Gantaohe group and the Hutuo group in the Wutai area, they proposed that the Guandu group's underlying strata must be Neoarchean in age.

We conducted a comprehensive study of the Huangcha Pluton, employing petrographical analysis, rock geochemical analysis, ICP-MS zircon U-Pb dating, and Nd isotope analysis. Our investigation aimed to elucidate the formation age, magma source, petrogenesis, and geodynamic setting of the Huangcha Pluton. By doing so, we sought to constrain the age of the Guandu group and offer compelling evidence for the evolutionary trajectory of the North China Craton.

2. Regional Geological Setting

The Zanhuang Complex, located in Hebei province, spans approximately 40–60 km in width from east to west and nearly 140 km in length from north to south, encompassing a total area of around 3850 km^2. Its principal configuration resembles a "spindle," trending in the NNE–SSW direction (Figure 1, adapted from [22,23]). Comprising a typical Pre-Cambrian metamorphic complex, the Zanhuang rock complex comprises late Archean TTG gneiss, potassic-two feldspar gneiss, the Zanhuang Complex, and the late Archeozoic—Paleo-Proterozoic Guandu group (Figure 1, [20,24–26]). To the west of this complex, it is unconformably overlain by the slightly metamorphic Gantaohe group, with localized fault contacts. To the south and west, it is unconformably covered by the Changcheng series, mid-Proterozoic strata. Numerous previous studies have focused on this rock complex [20,22–25,27–34]. Among them, the TTG gneiss primarily consists of tonalitic gneiss dated to approximately 2.7 billion years ago [26] and tonalitic-ganodioritic gneiss dated between 2.55 and 2.50 billion years ago [25,35].

All these gneisses are believed to have formed through plate melting processes in a subduction setting [25,26,35], while the potassic-two feldspar granitic gneiss serves as indicators for syn-collisional or post-collisional tectonic settings [25,35,36]. The Zanhuang group, appearing as fragments scattered within the TTG gneiss, comprises a suite of higher-grade metamorphic rock series primarily distributed in the western regions of the Huangshi town in the Xingtai city, the western parts of the Zhangmo village in the Neiqiu county, and around Huangbeipin of Zanhuang to Yuantou of Ningcheng. It is primarily composed of paragneiss, amphibolites, and metapelites, prominently featuring garnet-bearing kyanite plagioclase gneiss [37]. The Guandu group rocks exhibit clear stratification, forming a narrow NE–SW trending belt within the middle part of the Zanhuang Complex. They primarily consist of amphibolites, marble, quartzites, and early Proterozoic metapelites, with parent rock ages exceeding 2.5 billion years and having undergone amphibolite facies metamorphism approximately 1.8 billion years ago [33,38]. The Paleo-Proterozoic Gantaohe group is primarily distributed in the western regions of the Zanhuang Complex along both sides of the Gantaohe river basin, forming a north–south trending belt. It is also exposed in Shangzai of the Yuanshi county to Wujiayao, south of Jingjing, featuring abundant basic volcanic sedimentary rocks dated to 2090 million years ago and having undergone greenschist to lower amphibolite facies metamorphism [24,35,39,40].

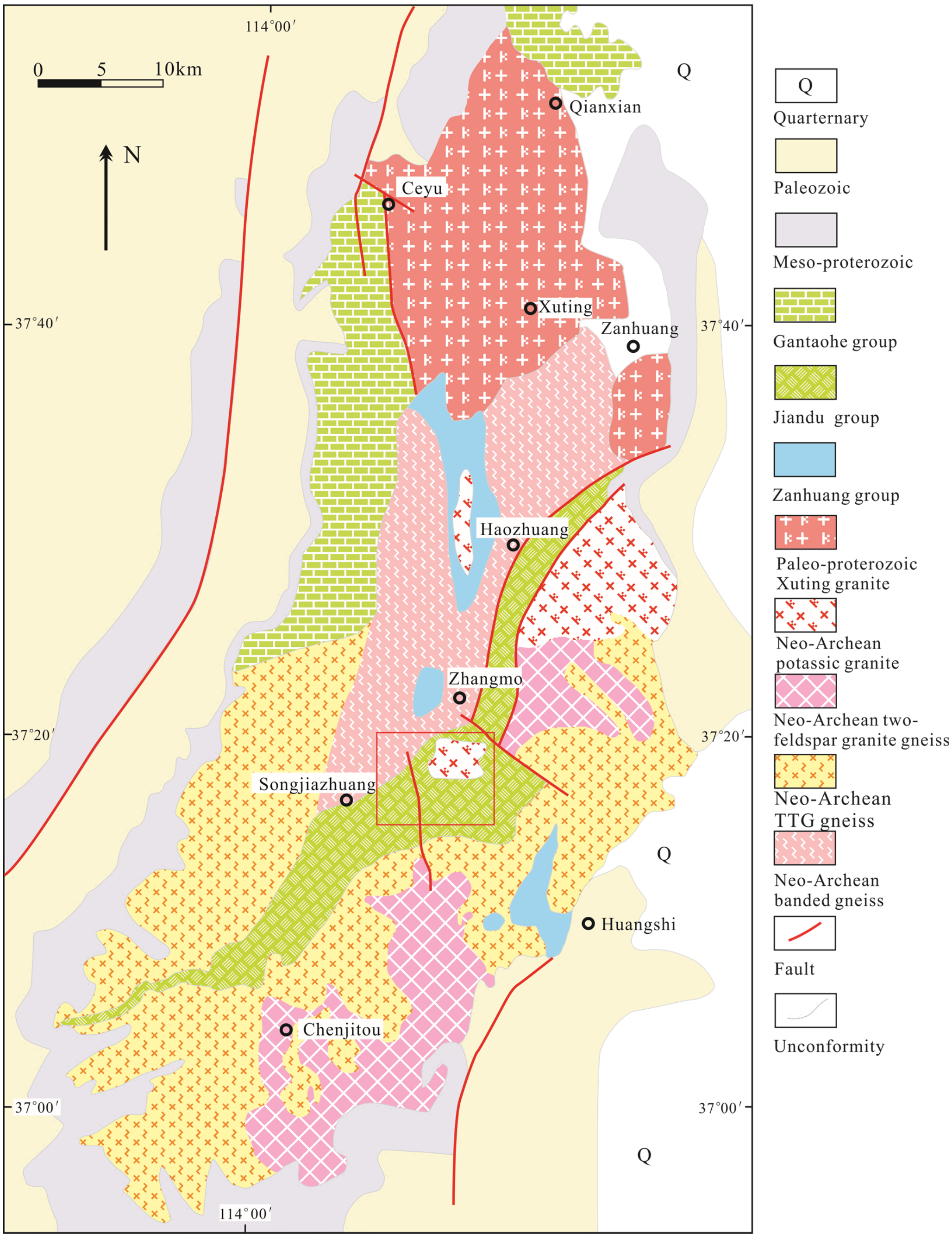

Figure 1. Geological sketch map of the Zanhuang Complex (Red box see Figure 2).

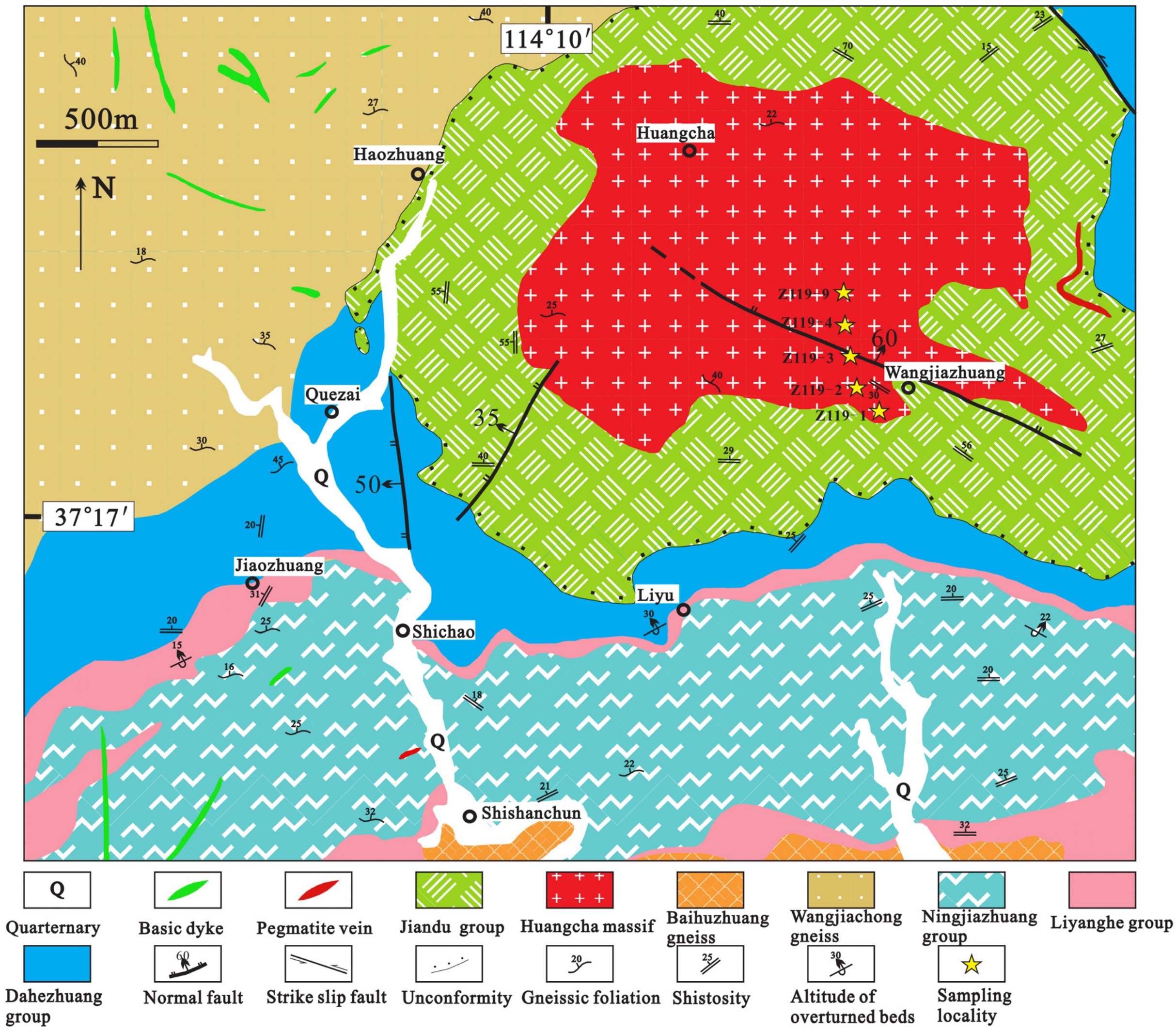

Figure 2. Geological sketch map of the Huangcha Pluton in the Zanhuang Complex.

Trap et al. [33] delineated the Zanhuang Complex into three divisions: east, central, and west. Along the western margin of the central division lies a significant tectonic suture zone. Their findings suggest that the formation of the Zanhuang Complex resulted from the collision and amalgamation of the eastern block of the North China Craton with the Fuping continental block along this tectonic suture zone 1880–1850 million years ago. Within the west division (WZD), the exposed formations primarily consist of TTG gneiss, migmatites, and anatectic granites. The central division (CZD) predominantly comprises quartz schist, volcanic sedimentary rock series, pelitic gneiss, orthogneiss-migmatite, and marble. Conversely, the east division (EZD) shares similarities with the west, featuring primarily TTG gneiss, pelitic gneiss, amphibolitic gneiss, and migmatites.

3. Petrography of the Huangcha Pluton

The Pluton manifests as towering, steep mountains with a distinct granite outlook (Figure 2). Its northern and southern portions are in fault contact with quartzites of the Guandu group, exhibiting a ductile shear zone structure where the foliation of the quartzites aligns with the gneissic foliation of the Pluton. The surface of the Huangcha Pluton presents a pink hue. Macroscopically, the rock appears homogeneous, characteristic of an intrusive rock (Figure 3a), with small amounts of fine-grained biotite plagioclase gneiss and medium-coarse-grained amphibole-biotite plagioclase gneiss enclaves visible (Figure 3b,c). The rocks predominantly exhibit a porphyritic texture and gneissic structure (Figure 3d), with the gneissic foliation attributed to later tectonic events. Intensive mylonitization is observed in the western margin of the Pluton. The rock composition is largely homogeneous, comprising mainly biotite two-feldspar granite with intersecting pegmatite veins. Notably, K-feldspar forms megacrysts dispersed within the biotite–quartz–plagioclase matrix (Figure 3e,f), contributing to the characteristic porphyritic texture of the rock.

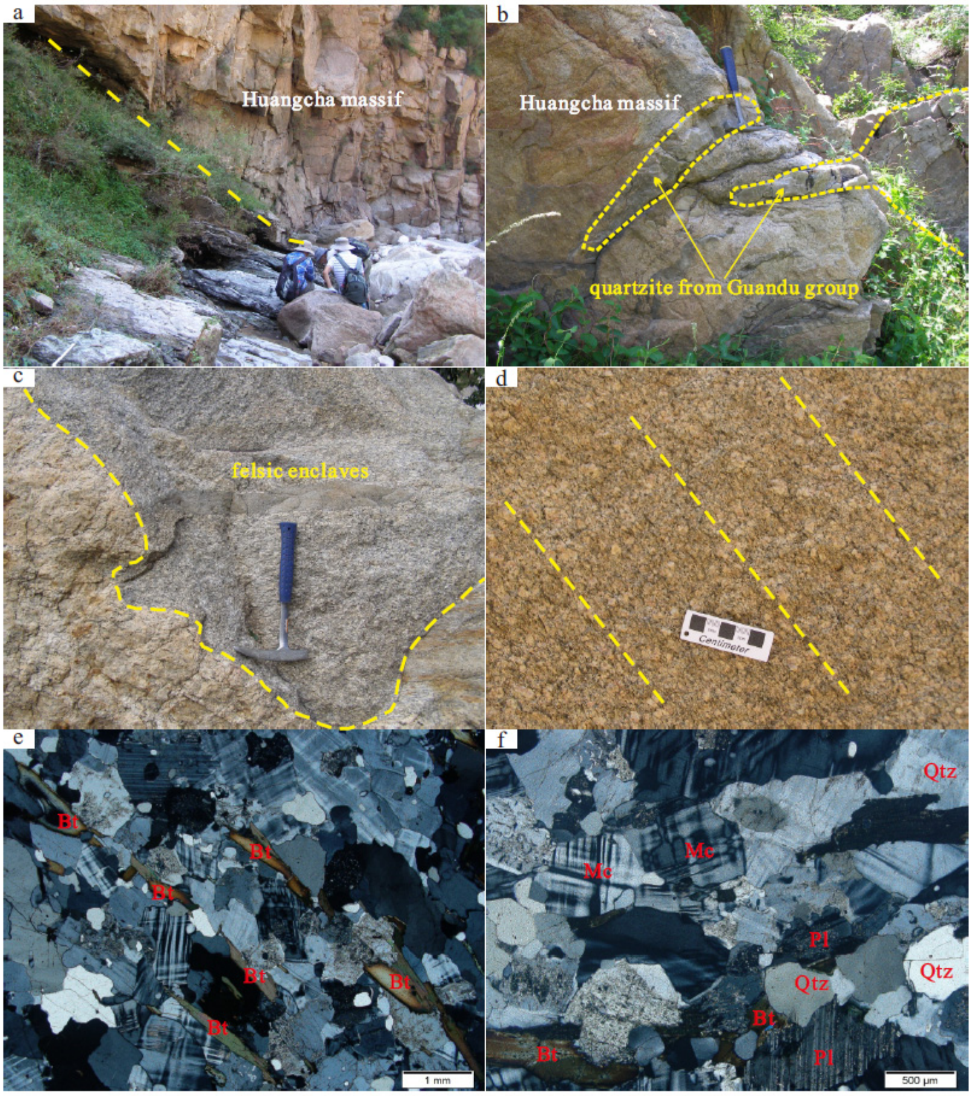

Figure 3. Field photos and photomicrographs of the Huangcha granite in the Zanhuang Complex. (**a**) The outlook of exposure; (**b**) Enclaves in the Pluton granite; (**c**) The felsic rock enclave; (**d**) Porphyroblastic texture and foliation (yellow lines); (**e**) Photomicrograph of the Huangcha granite; and (**f**) Myrmekite (upper left) in the Huangcha granite.

4. Analysis Methods

4.1. ICP-MS Zircon U-Pb Dating

We carried out ICP-MS zircon U-Pb dating, zircon Hf isotopic analysis, whole-rock geochemistry analysis, and whole-rock Sm-Nd isotopic analysis.

Zircon dating was conducted by the Isotope Laboratory of the Tianjin Institute of Geology and Mineral Resources using LA-MC-ICPMS to determine *in situ* U-Pb isotope in the micro-domain. The analysis apparatus was the Neptune-type MC-ICP-MS manufactured by the Thermo Fisher Company (Thermo Fisher Company, Waltham, MA, USA). The sample-entering laser apparatus matched with ICP-MS was the sub-molecule laser of UP193-FX ArF produced by the ESI company in the USA. The laser wavelength was

193 nm, and the impulse duration was 5 ns. The beam spot used in the test was 35 µm. The appropriate age-determining micro-domains in zircon were selected from CL images and from transmitted and reflected light micrographs. The ablation of zircon was conducted by a 193-nm laser. The U-Pb isotope diverse rectification was conducted by taking TEMORA and GJ-1 as the external standard of zircon dating [41,42]. The data processing was completed by using the ICP-MS DataCal program and the Ludwig Isoplot program [43]. The common lead rectification was conducted by using the ^{208}Pb Correction method [44]. The U, Pb, and Th contents of the zircon samples were calculated by using the NIST612 glass-type material as an external standard. LA-MC-ICPMS dating test conditions and key parameters: (1) receiving device—L4; ^{206}Pb; L3, ^{207}Pb; L2, ^{208}Pb; C, 219.26; H2, ^{232}Th; and H4, ^{238}U, (2) the cooling gas—^{206}Pb; L3, ^{207}Pb; L2, ^{208}Pb; C, 219.26; H2, ^{232}Th; and H4, ^{238}U, (3) the accessory gas: 0.75 L min^{-1}, (4) the loaded gas: 0.86 L·min^{-1}, (5) the RF power efficiency: 1251 W, (6) integral time: 0.131 s, and (7) sample signal collecting time: 60 s (including the empty testing time: 20 s).

4.2. Zircon Hf Isotopic Analysis

In situ zircon Hf isotopic analysis was conducted at the State Key Laboratory of Geological Processes and Mineral Resources, China University of Geosciences. Zircon Hf isotopes were analyzed using a Neptune Plus MC-ICP-MS (Thermo Fisher Company, Waltham, MA, USA) in combination with a Geolas 2005 excimer ArF laser ablation system with spot sizes of 44 µm and a laser pulse frequency of 8–10 Hz. The initial ^{176}Hf/^{177}Hf values of 0.282785 and ^{176}Lu/^{177}Hf values of 0.0336 were calculated with reference to the chondritic reservoir. Depleted mantle model ages (TDM) were calculated using values for the depleted mantle of ^{176}Hf/^{177}Hf = 0.28325 and ^{176}Lu/^{177}Hf = 0.0384. The Hf isotope crustal model ages (TDMC) were calculated by assuming that the samples' parental magma was derived from an average continental crust with a ^{176}Lu/^{177}Hf value of 0.015 and originated from a depleted mantle source [45].

4.3. Whole-Rock Geochemistry Analysis

Whole-rock geochemical analyses were conducted at the National Research Center for Geoanalysis, Beijing, China. Whole-rock major elements and trace elements including rare earth elements (REEs) were determined using standard X-ray fluorescence (XRF) and inductively coupled plasma mass spectrometry (ICP-MS) on a Finnigan MAT (Element I) instrument.

4.4. Whole-Rock Sm-Nd Isotopic Analysis

Sm and Nd were measured on a VG-354 TIMS (Thermo Fisher Company, Waltham, MA, USA) under standard operating conditions. The Nd isotopic standard, La Jolla, was measured in duplicate with each set of samples. Minor corrections were applied so that all data are reported relative to a value of 0.511860 for the 143Nd/144Nd ratio of the standard. Our 149Sm-150Nd isotopic tracer solution yielded a 147Sm/144Nd value of 0.196545 $\pm$ 15 for four analyses of the chondritic solution of natural Sm and Nd distributed by the California Institute of Technology.

5. Results of Geochemistry

5.1. Zircon U-Pb Ages

The zircon crystals selected for dating were obtained from rock sample Z119-1. These crystals exhibit euhedral to subhedral prismatic shapes, often displaying corroded pits on the surface, indicative of significant alteration during later geological events. The grain size of the zircon crystals mainly ranges from 100 to 300 µm, with a smaller proportion falling between 50 and 100 µm. The aspect ratios of the crystals are predominantly between 1.2 and 2.5, with a minor proportion ranging from 2.5 to 4. In the cathodoluminescence (CL) images, all the zircon crystals exhibit regular rhythmic zoning patterns (Figure 4), confirming their magmatic origin.

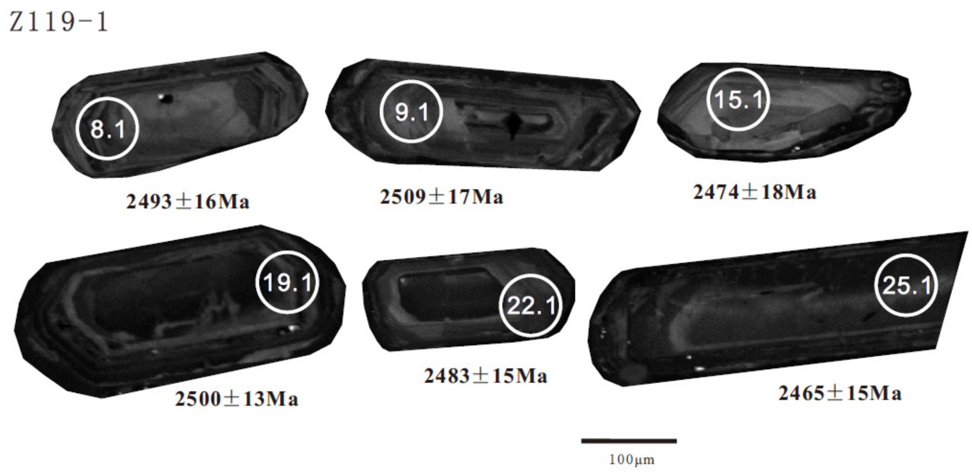

Figure 4. CL images of zircon from the Huangcha granite in the Zanhuang Complex.

A total of 31 measuring points were conducted for 31 zircon grains from the Huangcha Pluton (Z119-1). The U-Th content ranges from 13 to 109 ppm to 20 to 282 ppm, while the Th/U ratios range from 0.22 to 0.98 (refer to Table 1), characteristics typical of magmatic zircons. With the exception of two zircon analysis points showing a slight lead loss, all other analytical results are plotted on or near the concordia curve. Excluding the two points, namely 1.1 and 30.1, which yielded slightly smaller dating results, the remaining 29 analytical points yielded a $^{207}Pb/^{206}Pb$ weighted mean dating result of 2488 ± 6 Ma (MSWD = 1.11) (Figure 5). This age represents the crystalline age of zircon and signifies the formation age of the Huangcha Pluton.

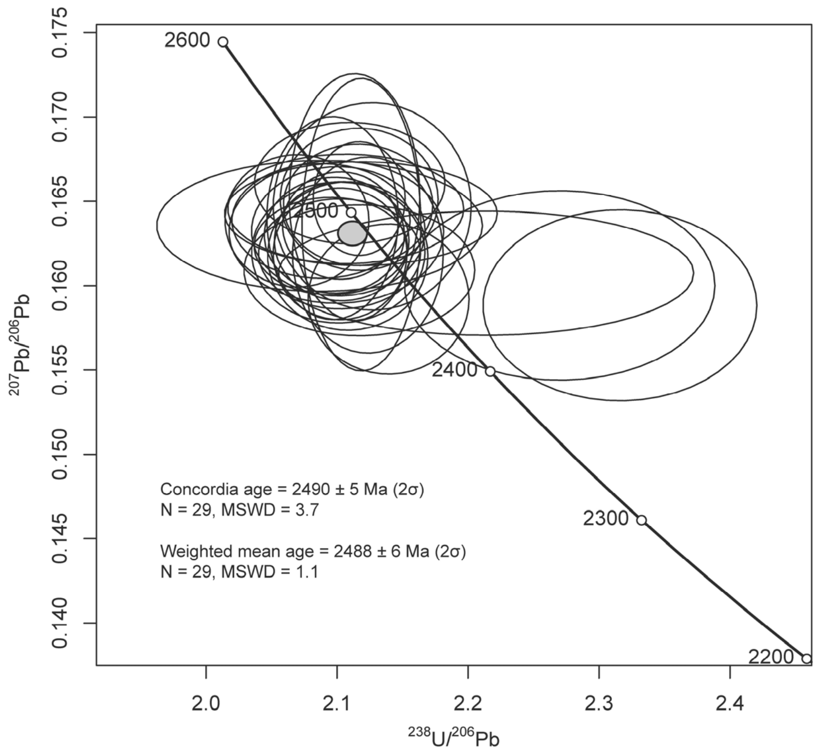

Figure 5. U-Pb Concordia age (TW diagram) of zircon from the Huangcha granite in the Zanhuang Complex.

Table 1. LA-ICP-MS U-Pb data of zircons from the Huangcha granite in the Zanhuang Complex.

Sample Number	Contents/ppm				Isotope Ratio						Age/Ma					
	Th	U	Pb	$\frac{Th}{U}$	$\frac{^{207}Pb}{^{206}Pb}$	1σ	$\frac{^{207}Pb}{^{235}U}$	1σ	$\frac{^{206}Pb}{^{238}U}$	1σ	$\frac{^{207}Pb}{^{206}Pb}$	1σ	$\frac{^{207}Pb}{^{235}U}$	1σ	$\frac{^{206}Pb}{^{238}U}$	1σ
Z119-1-1.1	27	122	41	0.22	0.14267	0.00166	5.99128	0.14347	0.30457	0.00808	2260	20	1975	47	1714	45
Z119-1-2.1	18	33	18	0.55	0.16401	0.00242	10.78591	0.17261	0.47697	0.00459	2497	25	2505	40	2514	24
Z119-1-3.1	13	20	11	0.68	0.16361	0.00349	10.64815	0.22762	0.47201	0.00407	2493	36	2493	53	2492	21
Z119-1-4.1	31	52	27	0.6	0.16001	0.00226	9.7188	0.23502	0.44053	0.00925	2456	24	2408	58	2353	49
Z119-1-5.1	97	171	95	0.56	0.16356	0.00128	10.72551	0.10925	0.47561	0.00402	2493	13	2500	25	2508	21
Z119-1-6.1	95	122	71	0.78	0.16516	0.00136	10.7574	0.10558	0.47239	0.00315	2509	14	2502	25	2494	17
Z119-1-7.1	24	32	18	0.76	0.1647	0.00247	10.67703	0.19799	0.47018	0.00672	2504	25	2495	46	2484	36
Z119-1-8.1	39	88	48	0.45	0.16355	0.00156	10.80649	0.2392	0.47923	0.01149	2493	16	2507	55	2524	60
Z119-1-9.1	31	52	29	0.6	0.16512	0.0017	10.75462	0.14698	0.47239	0.00541	2509	17	2502	34	2494	29
Z119-1-10.1	103	122	68	0.84	0.16074	0.00148	10.01161	0.21437	0.45172	0.01301	2463	16	2436	52	2403	69
Z119-1-11.1	18	24	13	0.76	0.16182	0.00234	10.50677	0.16056	0.47091	0.00513	2475	24	2481	38	2488	27
Z119-1-12.1	44	64	36	0.69	0.16299	0.00138	10.71201	0.1215	0.47665	0.00489	2487	14	2498	28	2513	26
Z119-1-13.1	36	55	31	0.65	0.16323	0.00154	10.71244	0.14755	0.47597	0.00604	2489	16	2499	34	2510	32
Z119-1-14.1	109	233	125	0.47	0.16235	0.00116	10.68397	0.11845	0.47728	0.00536	2480	12	2496	28	2515	28
Z119-1-15.1	36	39	23	0.93	0.16176	0.00177	10.57916	0.14868	0.47434	0.00554	2474	18	2487	35	2503	29
Z119-1-16.1	57	71	41	0.8	0.16385	0.00158	10.9172	0.13741	0.48323	0.00516	2496	16	2516	32	2541	27
Z119-1-17.1	34	42	24	0.81	0.1592	0.00179	10.26048	0.14385	0.46743	0.0054	2447	19	2459	34	2472	29
Z119-1-18.1	53	54	31	0.98	0.16189	0.00157	10.61718	0.1243	0.47566	0.00465	2475	16	2490	29	2508	24
Z119-1-19.1	81	143	79	0.56	0.16427	0.00124	10.69278	0.18047	0.4721	0.00933	2500	13	2497	42	2493	49
Z119-1-20.1	22	35	18	0.63	0.15883	0.00228	9.45579	0.18883	0.43179	0.00784	2443	24	2383	48	2314	42
Z119-1-21.1	56	82	46	0.68	0.16189	0.00131	10.61936	0.12655	0.47575	0.00563	2475	14	2490	30	2509	30
Z119-1-22.1	47	78	44	0.6	0.16264	0.00142	10.66003	0.12119	0.47538	0.00467	2483	15	2494	28	2507	25
Z119-1-23.1	44	63	36	0.69	0.16197	0.00168	10.62988	0.15319	0.47597	0.00603	2476	17	2491	36	2510	32
Z119-1-24.1	22	36	20	0.62	0.16525	0.00294	10.78138	0.19285	0.47319	0.00449	2510	30	2504	45	2498	24
Z119-1-25.1	59	98	55	0.6	0.16091	0.00156	10.47968	0.16662	0.47236	0.00791	2465	16	2478	39	2494	42
Z119-1-26.1	54	92	52	0.59	0.16479	0.00145	10.73752	0.12766	0.47257	0.00512	2505	15	2501	30	2495	27
Z119-1-27.1	40	74	41	0.53	0.16608	0.00145	10.8538	0.1457	0.474	0.00657	2518	15	2511	34	2501	35
Z119-1-28.1	56	95	54	0.59	0.16384	0.00137	10.82026	0.14871	0.47898	0.00628	2496	14	2508	34	2523	33
Z119-1-29.1	66	130	72	0.51	0.16455	0.00131	10.76981	0.17	0.47469	0.00816	2503	13	2503	40	2504	43
Z119-1-30.1	92	282	140	0.33	0.15569	0.00143	9.72079	0.2017	0.45283	0.00946	2409	16	2409	50	2408	50
Z119-1-31.1	41	80	44	0.52	0.16319	0.0017	10.71702	0.17807	0.47631	0.00748	2489	18	2499	42	2511	39

The five samples from the Huangcha Pluton were analyzed for major and trace element contents; the results and related parameters are shown in Table 2.

Table 2. Geochemical composition of the Huangcha granite in the Zanhuang Complex (major elements: ωt.% and rare earth and trace elements: ppm).

Sample Number	Z119-1	Z119-2	Z119-3	Z119-4	Z119-9
SiO_2	73.34	74.16	72.64	73.53	73.7
TiO_2	0.24	0.24	0.22	0.18	0.28
Al_2O_3	13.32	13.08	13.51	14.11	12.74
Fe_2O_3	2.71	2.64	2.43	1.84	3.03
MnO	0.04	0.03	0.03	0.02	0.06
MgO	0.31	0.46	0.38	0.34	0.38
CaO	1.18	0.82	0.67	1.67	1.1
Na_2O	3.1	2.94	2.92	4.06	2.75
K_2O	5.44	5.27	6.15	3.53	5.13
P_2O_5	0.06	0.06	0.05	0.05	0.07
LOI	0.5	0.51	0.53	0.45	0.38
TOTAL	100.24	100.21	99.53	99.78	99.62
ALK	8.54	8.21	9.07	7.59	7.88
A/NK	1.21	1.24	1.18	1.34	1.26
A/CNK	1.01	1.09	1.06	1.04	1.05
$Mg^{\#}$	19	26	24	27	20
TFeO/MgO	7.87	5.16	5.75	4.87	7.17
La	126	127	104	84	150
Ce	252	248	208	165	297
Pr	28.7	28.4	24	18.6	34.2
Nd	100.2	97.9	84.4	64.2	118.5
Sm	16.8	15.8	14.8	10.6	19.8
Eu	1.23	1.21	1.14	1.02	1.37
Gd	12.6	11.6	12.4	7.9	15.4
Tb	1.64	1.51	1.71	1.03	2.06
Dy	8.81	8.03	9.64	5.49	11.1
Ho	1.57	1.46	1.77	1.02	1.92
Er	4.39	4.08	4.81	2.9	4.91
Tm	0.61	0.57	0.66	0.41	0.62
Yb	3.79	3.63	4.02	2.62	3.61
Lu	0.56	0.53	0.58	0.38	0.51
ΣREE	558.9	549.72	471.93	365.17	661
δEu	0.25	0.26	0.25	0.33	0.23
$(La/Yb)_N$	23.89	25.07	18.65	22.83	29.82
Sc	4.57	4.78	4.19	2.47	7.68
V	5.77	6.33	5.19	10.08	7.21
Cr	2.38	2.95	1.43	5.69	2.06
Coi	1.63	1.68	1.58	1.8	2
Ni	1.72	2.06	1.19	3.1	1.46
Cu	3.96	4.1	5.45	12.67	5.05
Zn	63.6	55.6	51.1	39.4	66.1
Ga	21.6	20.5	20.9	20.5	20.9
Rb	254.5	236.1	271.4	156.2	223.2
Sr	109	108	100	214	124
Y	46.4	43.4	48.8	30.7	51.4
Zr	336	349	298	244	404
Nb	23.6	20	26.3	14.4	18.1
Cs	5.95	5.07	7.51	4.29	5.2
Ba	533	573	603	361	574
Hf	9.44	9.81	8.43	6.94	11.06
Ta	1.27	1.29	1.69	1.19	1.15
Pb	28.3	24.5	23.9	21.8	22.7
Th	31.8	29.2	25.9	21.2	34
U	3.03	2.34	2.33	2.56	2.9
Rb/Sr	2.34	2.19	2.72	0.73	1.8
Ca/Al	3.07	2.96	2.93	2.75	3.11
Y/Nb	1.96	2.17	1.86	2.12	2.84
Rb/Nb	10.77	11.82	10.33	10.81	12.32
Sc/Nb	0.19	0.24	0.16	0.17	0.42
T_{Zr} (°C)	687	689	694	660	699

5.2. Major Elements

The granites from the Huangcha Pluton are silica-rich (SiO_2 = 72.64%–74.16%), high in potassium (K_2O = 3.53%–6.15%), rich in alkaline compounds (ALK = 7.59%–9.07%), poor in calcium (CaO = 0.67%–1.67%), and low in titanium (TiO_2 = 0.18%–28%), magnesium (MgO = 0.31%–0.46%), and iron ($Fe_2O_3{}^T$ = 1.84%–3.03%) with higher TFeO/MgO ratio (4.87–7.87) but lower $Mg^{\#}$ value (19–27). Being correlated to high-silica rocks, the Pluton is higher in aluminum content (Al_2O_3 = 12.74%–14.11%) with an Al-saturated index A/CNK = 1.01–1.09, av. 1.05 and A/NK value ranging between 1.18 and 1.34; all of these show (weak) per-aluminous character (Figure 6a). K_2O contents are high in the rocks and are not correlated with SiO_2. On the SiO_2-K_2O plot, only one sample is plotted in the rock series of high K calc-alkaline and the other sample is plotted in the shoshonite rock series (Figure 6b). These major elements' characteristics sufficiently coincide with that of A-type granites [46–49].

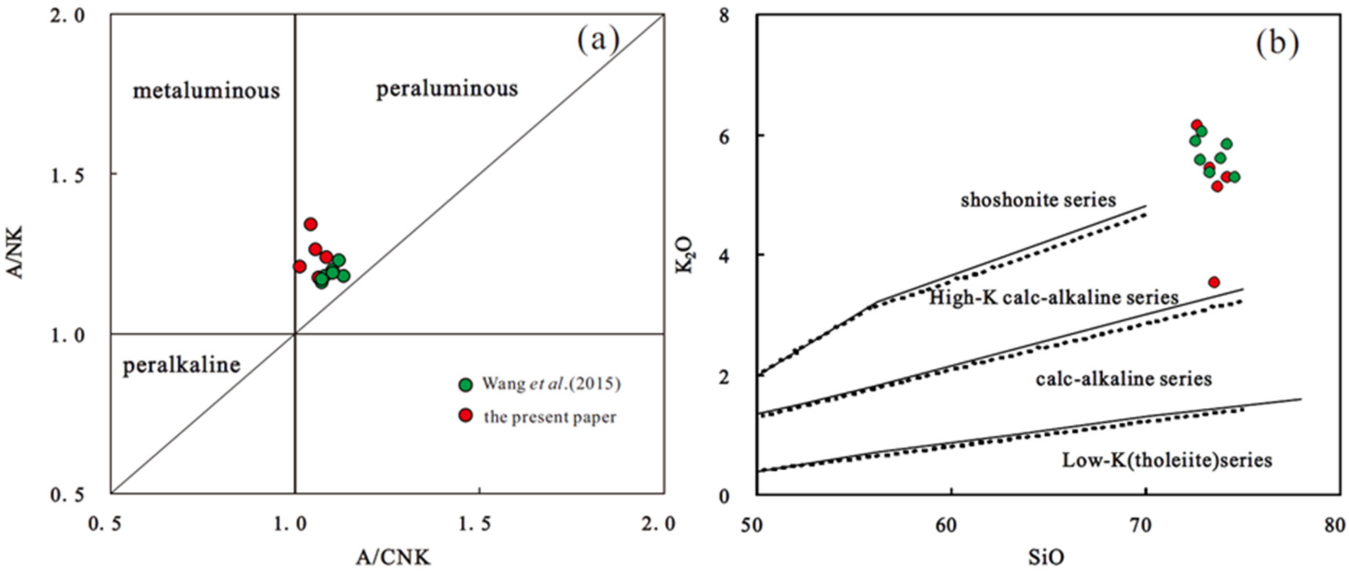

Figure 6. Geochemical diagrams of the Huangcha granite in the Zanhuang Complex. (**a**) A/NK-A/CNK and (**b**) SiO_2-K_2O [31].

5.3. REE and Trace Elements

The rocks in the Huangcha Pluton are high in REE content (Table 2) and vary greatly (ΣREE = 364.19–661.09 ppm, average of 521.19 ppm). In the chondrite-normalized distribution pattern, they show right-dipping "v" shaped curves (Figure 7a). ΣLREE is high, up to 342.44–620.93 ppm, av. of 488.61 ppm; ΣHREE is low: 21.74–40.15 ppm, av. of 32.58 ppm. The light and heavy REEs are moderately differentiated ($(La/Yb)_N$ = 17.57–28.1) with a prominent Eu anomaly (Eu/Eu* = 0.23–0.33). The REE characteristics are similar to those of A-type granites [46–49].

As for trace elements, the Huangcha Pluton rocks are high in Zr (244–404 ppm), Zn (39.4–66.1 ppm), Nb (14.4–26.3 ppm), Ga (20.5–21.6 ppm), and Y (30.7–51.4 ppm) but low in Sr, V, Cr, Co, and Ni. The rocks are low in Sr content (100–214 ppm, av. of 130.8 ppm) and high in Yb content (2.62–4.02 ppm, av. of 3.53 ppm). It is similar to the low Sr- and high Yb-type of granite (Sr < 400 ppm, Yb > 2 ppm) proposed by Zhang [50]. The primitive mantle-normalized spider diagram shows very clear negative anomalies of Ba, Sr, P, and Ti (Figure 7b). The Rb/Sr ratios of the samples are high, ranging between 0.73 and 2.72, with an average of 1.96, which is higher than the global upper crust average of 0.32. In addition, the Huangcha Pluton granites are high in Ga/Al ratio (2.75×10^{-4}–3.11×10^{-4}), which is higher than the lower limit of the A-type granite 2.6×10^{-4} [47]. In the discrimination diagrams of 10,000Ga/Al-($Na_2O + K_2O$) and 10,000Ga/Al-FeO*/MgO, they are plotted in the field of A-type granites (Figure 8).

In comparison to other types of granites, A-type granites are known to form at higher temperatures [51]. It is widely accepted that the saturation temperature of zircon can approximately represent the near-liquidus temperature of granitic rocks [52]. Since no residual zircon was found in samples from the Huangcha Pluton, the zircon saturation thermometer proposed by Watson and Harrison [52] can be applied in this case. The calculation indicates that the zircon saturation temperature of the Huangcha Pluton ranges between 826 and 877 °C, with an average of 853 °C (refer to Table 2). This temperature is notably higher than that of the S-type granite (average 764 °C) and I-type granite (average 781 °C) [51] and is comparable to that of typical A-type granites worldwide [53–57].

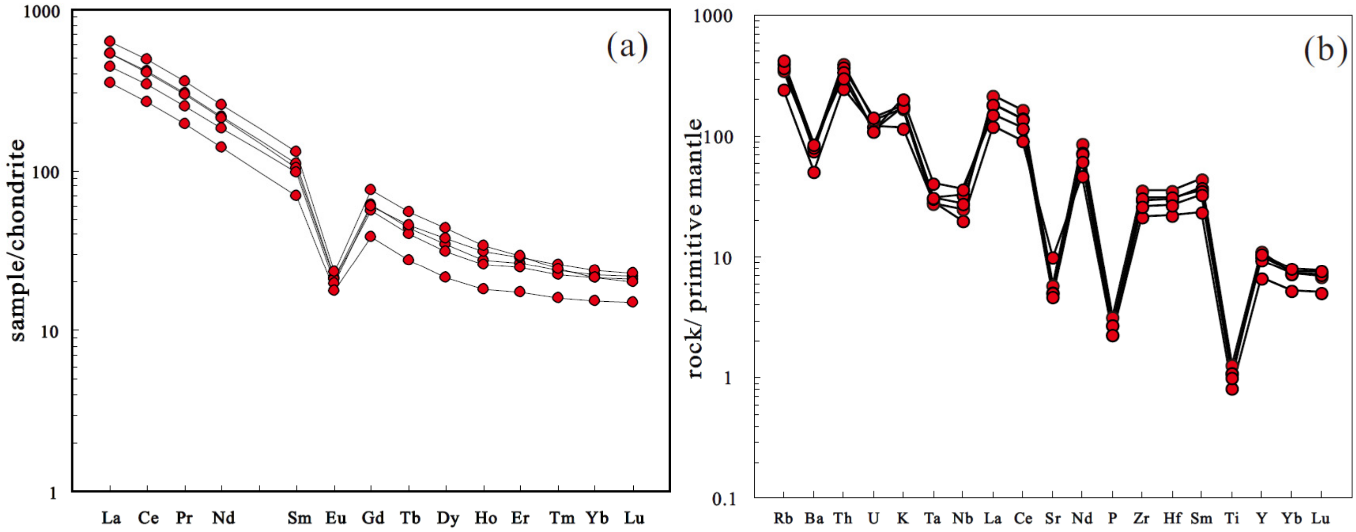

Figure 7. Chondrite-normalized REE distribution patterns (**a**) primitive mantle-normalized spidergrams [58] and (**b**) the Huangcha granite in the Zanhuang Complex.

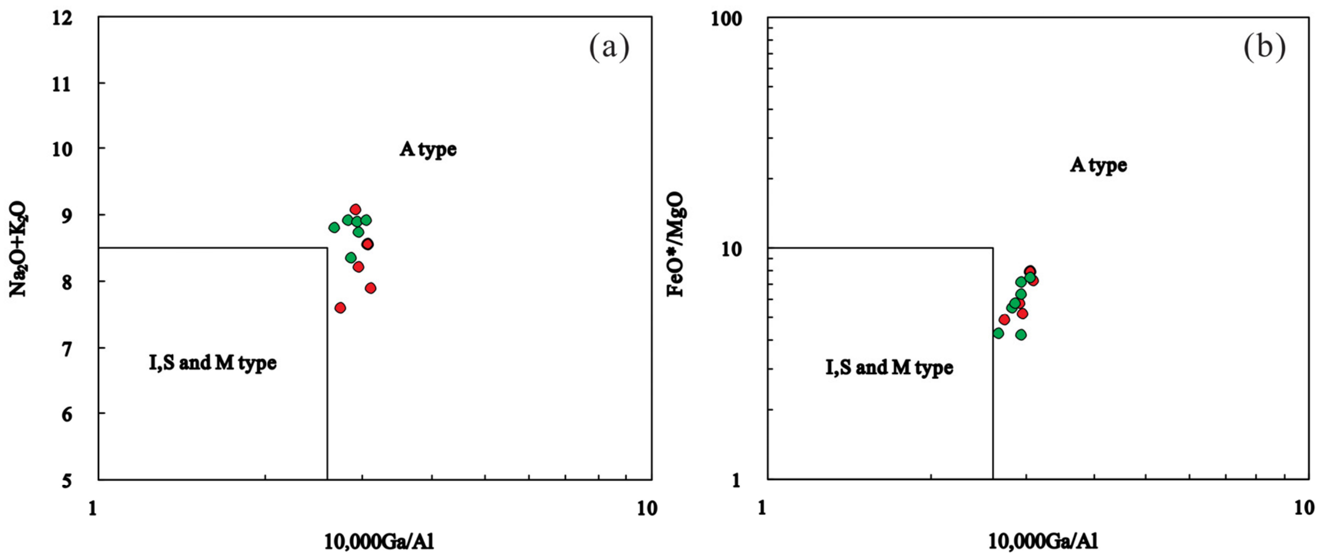

Figure 8. 10,000Ga/Al-($Na_2O + K_2O$) (**a**) and 10,000Ga/Al-FeO*/MgO (**b**) diagrams of the Huangcha granite in the Zanhuang Complex (Green circle data from [31], red circle data from the present paper, base diagram from [47]).

5.4. Isotope Geochemistry

Wang et al. [36] conducted Sm-Nd isotope analyses for the Huangcha Pluton. In the present paper, the $(^{143}Nd/^{144}Nd)_I$ values from the above analyses are recalculated according to our new yielded age (2488 Ma); the results are shown in Table 3. The $\varepsilon Nd(t)$ values range between −0.06 and 0.88, the single-stage depleted mantle model age t_{DM1} ranges between 2746 and 2851 Ma, and the two-stage depleted mantle model age t_{DM2} ranges between 2790 and 2867 Ma, with an average of 2829 Ma. The $f_{Sm/Nd}$ values of samples are slightly varying negative numbers (−0.41–−0.47), indicating that the fractionation of Sm-Nd in the source area is not significant; therefore, the calculated Nd model age is geologically reasonable.

Table 3. Sm-Nd isotopic composition of the Huangcha granite in the Zanhuang Complex.

Sample Number	Sm ppm	Nd ppm	$^{147}Sm/^{144}Nd$	$^{143}Nd/^{144}Nd$	$\varepsilon_{Nd}(t)$	$f_{Sm/Nd}$	T_{DM1} (Ma)	T_{DM2} (Ma)
13XT-17-1	8.78	45.6	0.116	0.511311	−0.06	−0.41	2851	2867
13XT-19-1	13.1	72.3	0.110	0.511236	0.40	−0.44	2796	2829
13XT-22-1	14.3	83.0	0.104	0.511162	0.88	−0.47	2746	2790

Representative thirty-one zircon grains of sample Z119-1 were analyzed for Lu-Hf isotopes, and the result is shown in Table 4. The data show that all the $^{176}Lu/^{177}Hf$ ratios are less than 0.002, indicating the absence of any major enrichment of radiogenic Hf after the formation of the zircons. All the zircon grains exhibit $^{176}Hf/^{177}Hf$ ratios varying from 0.281266 to 0.281412 and εHf(*t*) values ranging from 0.96 to 6.18 calculated with the $^{207}Pb/^{206}Pb$ age. Their Hf depleted mantle model ages (T_{DM}) and Hf crust model ages (T_{DM}^{C}) range from 2552 to 2746 Ma and 2576 to 2826 Ma, respectively (Table 4, Figure 9). It is suitable with the calculated age of 2.85 to 2.70 Ga based on εHf(*t*) values of 1.36 to 6.37 in the Guandu group [19]. This age period represents the strongest crustal growth stage in the Zanhuang region.

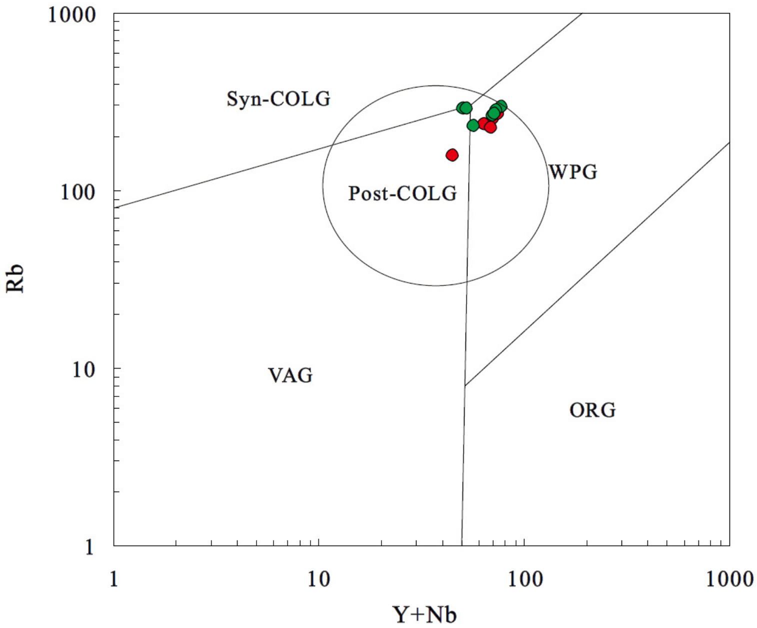

Figure 9. Rb versus (Y + Nb) tectonic discrimination diagram of the Huangcha granite in the Zanhuang Complex (Green circle data from [31], red circle data from the present paper, base diagram from [59]).

Table 4. Lu-Hf isotopic composition of the Huangcha granite in the Zanhuang Complex.

Sample No.	Age (Ma)	$\frac{^{176}Yb}{^{177}Hf}$	2σ	$\frac{^{176}Lu}{^{177}Hf}$	2σ	$\frac{^{176}Hf}{^{177}Hf}$	2σ	$f_{Lu/Hf}$	$(\frac{^{176}Hf}{^{177}Hf})_i$	$\varepsilon_{Hf}(0)$	$\varepsilon_{Hf}(t)$	T_{DM1} (Ma)	T_{DM2} (Ma)
Z119-1-1	2488	0.032454	0.000153	0.000924	0.000011	0.281333	0.000024	−0.97	0.281293	−50.9	3.40	2671	2726
Z119-1-2	2497	0.022479	0.000422	0.000567	0.000012	0.281308	0.000023	−0.98	0.281281	−51.8	3.32	2680	2736
Z119-1-3	2493	0.026414	0.000129	0.000656	0.000001	0.281339	0.000028	−0.98	0.281308	−50.7	4.18	2644	2690
Z119-1-4	2456	0.026486	0.000182	0.000634	0.000004	0.281305	0.000026	−0.98	0.281275	−51.9	2.15	2689	2760
Z119-1-5	2493	0.021348	0.000121	0.000596	0.000004	0.281290	0.000022	−0.98	0.281261	−52.4	2.53	2706	2772
Z119-1-6	2509	0.051520	0.000519	0.001373	0.000019	0.281388	0.000026	−0.96	0.281323	−48.9	5.08	2626	2660
Z119-1-7	2504	0.017138	0.000253	0.000470	0.000004	0.281327	0.000026	−0.99	0.281304	−51.1	4.33	2648	2692
Z119-1-8	2493	0.018982	0.000541	0.000547	0.000012	0.281285	0.000024	−0.98	0.281258	−52.6	2.42	2710	2777
Z119-1-9	2509	0.014960	0.000122	0.000441	0.000002	0.281296	0.000024	−0.99	0.281274	−52.2	3.36	2688	2743
Z119-1-10	2463	0.037490	0.000212	0.001028	0.000004	0.281334	0.000020	−0.97	0.281286	−50.9	2.71	2677	2740
Z119-1-11	2475	0.019832	0.000060	0.000578	0.000003	0.281369	0.000023	−0.98	0.281341	−49.6	4.96	2599	2637
Z119-1-12	2487	0.020805	0.000224	0.000633	0.000005	0.281274	0.000020	−0.98	0.281244	−53.0	1.79	2730	2804
Z119-1-13	2489	0.016638	0.000301	0.000506	0.000006	0.281295	0.000022	−0.98	0.281271	−52.2	2.78	2693	2756
Z119-1-14	2480	0.022341	0.000150	0.000695	0.000003	0.281266	0.000021	−0.98	0.281233	−53.3	1.22	2746	2826
Z119-1-15	2474	0.025736	0.000129	0.000751	0.000001	0.281412	0.000023	−0.98	0.281376	−48.1	6.18	2552	2576
Z119-1-16	2496	0.023113	0.000061	0.000701	0.000001	0.281331	0.000019	−0.98	0.281297	−51.0	3.87	2659	2708
Z119-1-17	2447	0.018915	0.000104	0.000587	0.000005	0.281274	0.000022	−0.98	0.281247	−53.0	0.96	2727	2812
Z119-1-18	2475	0.027822	0.000063	0.000847	0.000002	0.281306	0.000019	−0.97	0.281266	−51.9	2.28	2702	2770
Z119-1-19	2500	0.016027	0.000178	0.000548	0.000005	0.281275	0.000018	−0.98	0.281249	−52.9	2.26	2722	2791
Z119-1-20	2443	0.020797	0.000213	0.000697	0.000006	0.281311	0.000022	−0.98	0.281278	−51.7	1.99	2685	2758
Z119-1-21	2475	0.013688	0.000072	0.000466	0.000002	0.281292	0.000019	−0.99	0.281270	−52.3	2.43	2694	2762
Z119-1-22	2483	0.014937	0.000075	0.000508	0.000001	0.281298	0.000018	−0.98	0.281274	−52.1	2.77	2689	2752
Z119-1-23	2476	0.014070	0.000100	0.000465	0.000002	0.281370	0.000022	−0.99	0.281348	−49.6	5.22	2590	2624
Z119-1-24	2510	0.016536	0.000125	0.000513	0.000002	0.281357	0.000022	−0.98	0.281332	−50.1	5.45	2610	2641
Z119-1-25	2465	0.028944	0.000364	0.000871	0.000008	0.281326	0.000019	−0.97	0.281285	−51.1	2.74	2676	2739
Z119-1-26	2505	0.019425	0.000108	0.000652	0.000002	0.281337	0.000020	−0.98	0.281306	−50.8	4.40	2646	2689
Z119-1-27	2518	0.020775	0.000126	0.000629	0.000002	0.281350	0.000023	−0.98	0.281319	−50.3	5.19	2628	2661
Z119-1-28	2496	0.015382	0.000176	0.000463	0.000004	0.281339	0.000021	−0.99	0.281317	−50.7	4.57	2631	2672
Z119-1-29	2503	0.017225	0.000253	0.000515	0.000005	0.281320	0.000018	−0.98	0.281295	−51.4	3.96	2661	2709
Z119-1-30	2409	0.016187	0.000294	0.000513	0.000006	0.281320	0.000016	−0.98	0.281296	−51.4	1.84	2660	2737
Z119-1-31	2489	0.015532	0.000141	0.000454	0.000002	0.281271	0.000017	−0.99	0.281249	−53.1	2.01	2722	2793

Note: For data with strong lead loss, calculate the Hf homology of zircon using the weighted average age of the rock mass.

6. Discussion

6.1. The Age of the Guandu Group

The Guandu group comprises clearly layered metamorphic strata that were dismembered from the Zanghuang group. It predominantly consists of various schists and marble formations [35]. Initially named the Guandu formation during a regional geological survey in 1990 at a scale of 1:50,000; it was later officially designated as the Guandu group on the 1:500,000 Geological Map of Hebei province. Field observations have established that the Huangcha Pluton intruded into the Guandu group, allowing for the determination of the latest forming age of the Guandu group. Wang et al. [36] reported that three samples from the Huangcha Pluton yielded a weighted mean age of approximately 2.5 Ga. In this study, the zircon ICP-MS U-Pb dating of the Huangcha Pluton provided an age of 2488 $\pm$ 6 Ma. Consequently, the author concludes that the age of the Guandu group should be Neoarchean.

6.2. Source of Magma and Petrogenesis

As discussed earlier, the geochemical characteristics of the Huangcha Pluton granite, along with its notably high Zr saturation temperature, suggest its classification as A-type granite. Several petrogenetic models for A-type granite have been proposed, including (1) direct differentiation from mantle alkaline basaltic magma [60–65]; (2) partial melting of dry felsic granulite relicts enriched in F or Cl in the lower crust [46,47,54]; and (3) magma mixing between granitic magma and mantle-derived basaltic magma [66–68]. Considering the major elemental composition of the Huangcha Pluton granite, which is notably high in silica, rich in potassium, and depleted in magnesium and chromium, direct derivation from the mantle seems unlikely. Experimental evidence provided by [69–71] suggested that granites formed through partial melting of dry felsic granulite relicts enriched in F or Cl in the lower crust should exhibit characteristics inconsistent with those observed in the Huangcha Pluton granite, such as relative richness in Ca, Al, Mg, and Fe and depletion in K and Si. Moreover, the absence of chilled fine-grain mantle-derived enclaves in the petrographic features of the Huangcha granite argues against a magma mixing process. Additionally, considering the high $\varepsilon Nd(t)$ value, if mantle-derived magma assimilated with crust or underwent magma mixing with crust-derived magma, a significant addition of mantle material would be expected, leading to the formation of Nd isotopic characteristics contrary to those observed in the rock. Therefore, the evidence suggests that the Huangcha Pluton granite did not form through a magma mixing process between granite magma and mantle-derived basic magma.

Indeed, numerous experimental findings have supported the notion that A-type granites are likely generated through the partial melting of TTG (Tonalite–Trondhjemite–Granodiorite) and quartz diorite under conditions of high temperature and low pressure. In the Zanhuang area, there are extensive occurrences of Neoarchean TTG gneiss, whose age aligns with the predominant Nd model age of the Huangcha granite. TTG rocks are directly derived from the partial melting of mantle-derived basaltic rocks, inheriting many characteristics of mantle rocks, including relatively high $\varepsilon Nd(t)$ values. Hence, we propose that the Huangcha granites were formed through a partial melting process of Neoarchean TTG rocks. The $\varepsilon Nd(t)$ value close to 0 suggests that the juvenile TTG had not resided in the crust for an extended period, further supporting this proposed formation mechanism [72–76].

6.3. Tectonic Setting

A-type granite represents a distinct type of granite characteristic of extensional tectonic settings, which can encompass post-orogenic extensional settings or non-orogenic rift environments, such as intracontinental rifts or back-arc basins. In the tectonic discrimination diagram of granites proposed by [59], the Huangcha granite plot within the field was associated with post-collisional tectonics (Figure 10). Further subdivision in the tectonic setting correlation diagram for A-type granites places the Huangcha granites within the A2-type category, specifically indicating a post-orogenic extensional setting.

Notably, these granites exhibit low Sr and high Yb contents, characteristics often associated with formation under low-pressure conditions (less than 0.8 or 1.0 GPa) within a crust of normal thickness (approximately 30 km). Based on this understanding, it is inferred that the Huangcha Pluton granite formed within a context of initial crustal extensional thinning following compressive collisional orogeny. This interpretation finds support in the formation of the Jiandeng Pluton, reported by [72], which formed in a transitional tectonic setting between compressive collisional orogeny and post-orogenic extensional settings around 2490 ± 13 Ma. Given the temporal sequence, with the Huangcha Pluton being later than the Jiandeng Pluton, this inference appears logically consistent.

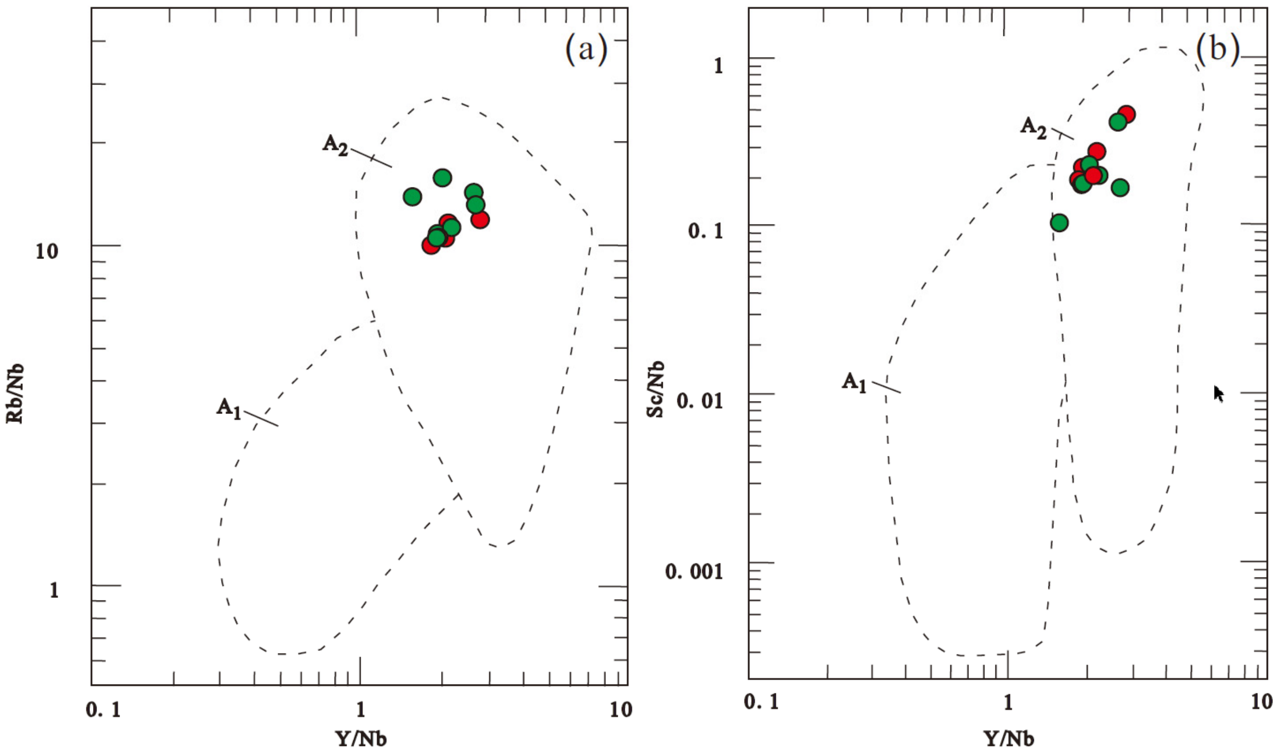

Figure 10. Rb/Nb versus Y/Nb (**a**) and Sc/Nb versus Y/Nb (**b**) tectonic discrimination diagrams of the Huangcha granite in the Zanhuang Complex (Green circle data from [31], red circle data from the present paper, base diagram from [74]).

The magmatic rocks in the age around 2.5 Ga are widely developed in the North China Craton, which are mainly shown as granitic intrusions spreading over the eastern block and the central tectonic belt, having similar geochemistry and probably being formed in similar tectonic settings [36]. However, the understanding of the character of the granitic rocks is still open for debate. Although some authors considered that it must be related to the underplating of the mantle plume [77–80], others suggested that these granites can be the products of partial melting of ancient TTG rocks from the lower crust in the island-arc tectonic setting related to subduction [8,9,12,20,33,76,81–95]. Combined with the studies on magma source and petrogenesis, the present paper further confirmed the viewpoint proposed by Yang [20], i.e., before the formation of the Huangcha Pluton granite, the stable craton had been formed, the Paleo-Proterozoic magmatic activity developed in this area has also proved this point of view [20,96–101]. In addition, the magmatism and metamorphic event in about 1.8 Ga recorded the time for the Paleo-Proterozoic intracontinental matching of the North China Craton.

6.4. Implications for Global Correlation

The analysis of the global craton evolution history suggests that there were three types of craton groups in the Paleoarchean: Superia, Vaalbara, and Nunavutia (also known as

Rae) craton groups [102]. The Superia family mainly includes the Karelia, Superior, and Wyoming cratons, which formed the Superia supercraton around ~2.7 Ga. The Kaapvaal and Pilbara cratons likely formed the Vaalbara supercraton around ~2.8 Ga. The North China Craton, along with the Congo, West African, Siberian, and Rae cratons, likely formed the Nunavutia supercraton around ~2.5 Ga. Our results support the cratonization of the North China Craton around ~2.5 Ga, with a similar evolutionary history to the Rae-family cratons. The research findings support the affinity of these cratons from the late Neoarchean to the early Paleo-Proterozoic, sharing similar magmatic and tectonometamorphic records around ~2.5 Ga.

7. Conclusions

1. The LA-ICP-MS zircon U-Pb dating yields the age of the Huangcha Pluton granite as 2488 ± 6 Ma, which shows that the age of the Guandu group should be Neoarchean.
2. The major element geochemistry of the Huangcha granite shows that it is rich in silica, high in potassium, rich in alkaline compounds, and low in calcium, titanium, magnesium, and iron; the fractionation between LREE and HREE is intermediate with a clear negative Eu anomaly; it is high in Zr, Zn, Nb, Ga, and Y but low in Sr, V, Cr, Co, and Ni, with a high Rb/Sr ratio and εNd(t) value close to 0, indicating typical characteristics of A-type granite.
3. The Huangcha Pluton granite is formed from partial melting of the juvenile crust with short crustal residence and was formed in a preliminary extensional tectonic setting after compressive collisional orogeny, which indicates that at the end of the Neoarchean, the North China Craton had already primarily undergone cratonization.

Author Contributions: S.C.: Conceptualization, Methodology, Validation, Formal analysis, Investigation, Data curation, and Writing—original draft. L.L.: Conceptualization, Validation, and Formal analysis. C.Y.: Methodology, Validation, Formal analysis, Supervision, and Funding acquisition. Y.Y.: Conceptualization, Methodology, Validation, Formal analysis, Investigation, Data curation, Writing—original draft, and Supervision. All authors have read and agreed to the published version of the manuscript.

Funding: This study was supported by the Natural Science Foundation (Grant No. 41572175), China Nuclear Uranium Co., Ltd. with the East China University of Technology (Grant No. 2023NRE-LH06), and a special program from the Geological Survey of China (DD20160121-04).

Data Availability Statement: Data are contained within the article.

Acknowledgments: We are thankful to Derek A. Wyman of the University of Sydney for his valuable help with the revision of this manuscript.

Conflicts of Interest: Lun Li is an employee of Beijing Jingneng Geological Engineering Co., Ltd. The paper reflects the views of the scientists and not the companies.

References

1. Brown, M.; Johnson, T. Secular change in metamorphism and the onset of global plate tectonics. *Am. Mineral.* **2018**, *103*, 181–196. [CrossRef]
2. Cawood, P.A.; Hawkesworth, C.J.; Pisarevsky, S.A.; Dhuime, B.; Capitanio, F.A.; Nebel, O. Geological archive of the onset of plate tectonics. Philos. Trans. *Am. Math. Phys. Eng. Sci.* **2018**, *376*, 20170405.
3. Condie, K.C. A planet in transition: The onset of plate tectonics on Earth between 3 and 2 Ga? *Geosci. Front.* **2018**, *9*, 51–60. [CrossRef]
4. Hawkesworth, C.J.; Cawood, P.A.; Dhuime, B. The Evolution of the Continental Crust and the Onset of Plate Tectonics. *Front. Earth Sci.* **2020**, *8*, 326. [CrossRef] [PubMed]
5. Zhao, G.C.; Cawood, P.A.; Wilde, S.A. Metamorphism of basement rocks in the Central Zone of the North China Craton: Implications for Paleoproterozoic tectonic evolution. *Precambr. Res.* **2000**, *103*, 55–88. [CrossRef]
6. Regelous, A.; Scharfenberg, L.; Wall, H.D. Origin of S-, A- and I-Type Granites: Petrogenetic Evidence from Whole Rock Th/U Ratio Variations. *Minerals* **2021**, *11*, 672. [CrossRef]
7. Zhao, G.C.; Wilde, S.A.; Cawood, P.A. Archean blocks and their boundaries in the North China Craton: Lithological, geochemical, structural and P-T path constraints and tectonic evolution. *Precambr. Res.* **2001**, *107*, 45–73. [CrossRef]

8. Zhao, G.C.; Wilde, S.A.; Cawood, P.A. SHRIMP U-Pb zircon ages of the Fuping Complex: Implications for Late Archean to Paleoproterozoic accretion and assembly of the North China Craton. *Am. J. Sci.* **2002**, *302*, 191–226. [CrossRef]
9. Zhao, G.C.; Sun, M.; Wilde, S.A. Late Archean to Paleoproterozoic evolution of the North China Craton: Key issues revisited. *Precambr. Res.* **2005**, *136*, 177–202. [CrossRef]
10. Li, J.H.; Qian, X.L.; Huang, X.N. Tectonic framework of North China Block and its cratonization in the Early Precambrian. *Acta Petrol. Sinica* **2000**, *16*, 1–10, (In Chinese with English Abstract).
11. Li, J.H.; Niu, X.L.; Kusky, T.M. Neoarchean plate tectonic evoluation of North China and its correlation with global cratonic blocks. *Earth Sci. Front.* **2004**, *11*, 273–283, (In Chinese with English Abstract).
12. Li, J.H.; Hou, G.T.; Liu, S.J. The Early Precambrian collisional orogenic process and plate tectonics: Chance and challenge of Precambrian geology. *Adv. Earth Sci.* **2006**, *21*, 77–82, (In Chinese with English Abstract).
13. Kusky, T.M.; Li, J.H. Paleoproterozoic tectonic evolution of the North China Craton. *J. Asian Earth Sci.* **2003**, *22*, 383–397. [CrossRef]
14. Kusky, T.M.; Li, J.H.; Santosh, M. The Paleoproterozoic North Hebei Orogen: North China Craton's collisional suture with the Columbia supercontinent. *Gondwana Res.* **2007**, *12*, 4–28. [CrossRef]
15. Wang, Z.H. Tectonic evolution of the Hengshan–Wutai–Fuping complexes and its implication for the Trans-North China Orogen. *Precambr. Res.* **2009**, *170*, 73–87. [CrossRef]
16. Wang, Z.H.; Wilde, S.A.; Wan, J.L. Tectonic setting and significance of 2.3-2.1 Ga magmatic events in the Trans-North China Orogen:New constraints from the Yanmenguan mafic-ultramafic intrusion in the Hengshan-Wutai-Fuping area. *Precambr. Res.* **2010**, *178*, 27–42. [CrossRef]
17. Xiao, D.; Ning, W.B.; Wang, J.P. Neoarchean to Paleoproterozoic tectonothermal evolution of the North China Craton: Constraints from geological mapping and Th-U-Pb geochronology of zircon, titanite and monazite in Zanhuang Pluton. *Precambr. Res.* **2021**, *359*, 105–214. [CrossRef]
18. Shi, K.X.; Wang, C.M.; Du, B.; Chen, Q.; Zhu, J.X. Neoarchean to Palaeoproterozoic tectonic evolution of theTrans-North China Orogen, North China Craton: Evidence fromzircon U-Pb geochronology, Lu–Hf isotopes, and geochemistryof the Zanhuang Complex. *Geol. J.* **2021**, *56*, 1236–1257. [CrossRef]
19. Liu, P.H.; Yang, C.H.; Du, L.L.; Tian, Z.H.; Zou, L.; Wang, Y.L.; Zhang, Y.J. Depositional age and provenance of the Guandu Group in the Zanhuang Complex, North China Craton: Constraints from detrital zircon U-Pb-Hf isotopic and rare earth element compositions in the biotite leptynite and quartzite. *Acta Petrol. Miner.* **2022**, *41*, 247–286, (In Chinese with English Abstract).
20. Yang, C.H.; Du, L.L.; Ren, L.D. The age and petrogenesis of the Xuting granite in the Zanhuang Complex, Hebei Province: Constraints on the structural evolution of the Trans-North China Orogen, North China Craton. *Acta Petrol. Sinica* **2011**, *27*, 1003–1016, (In English with Abstract).
21. Wang, J.P.; Kusky, T.M.; Wang, L. A Neoarchean subduction polarity reversal event in the North China Craton. *Lithos* **2015**, *220–223*, 133–146. [CrossRef]
22. Niu, S.Y.; Chen, L.; Xu, C.S. *The Crustal Evolution and Metallogenic Regularity of the Taihangshan Area*; Seismic Publishing House: Beijing, China, 1994; pp. 1–90. (In Chinese)
23. Niu, S.Y.; Xu, C.S.; Guo, L.J. The study of origin and characteristics of the Taihangshan metamorphic core complexes. *J. Hebei Coll. Geol.* **1994**, *17*, 43–53, (In Chinese with English Abstract).
24. Bureau of Geology and Mineral Resources of Hebei Province (BGMRHP). *Regional Geology of Beijing, Tianjin and Hebei Province*; Geological Publishing House: Beijing, China, 1989; pp. 16–30, 347–351, 353–354. (In Chinese)
25. Yang, C.H.; Du, L.L.; Ren, L.D. Petrogenesis and geodynamic setting of Jiandeng potassic granite at the end of the Neoarchean in the Zanhuang Complex, North China Craton. *Earth Sci. Front.* **2011**, *18*, 62–78, (In English with Abstract).
26. Yang, C.H.; Du, L.L.; Ren, L.D. Delineation of the ca. 2.7 Ga TTG gneisses in the Zanhuang Complex, North China Craton and its geological implications. *J. Asian Earth Sci.* **2013**, *72*, 178–189. [CrossRef]
27. Lei, S.H.; Hu, S.J. Models for Fuping-Zanhuang metamorphic core complex structure, Hebei, China. *J. Hebei Coll. Geol.* **1994**, *17*, 54–64, (In Chinese with English Abstract).
28. Wang, Y.J.; Fan, W.M.; Guo, F. Biotite $^{40}Ar/^{39}Ar$ geochronology of the deformational rocks from Zanhuang metamorphic domin in south Taihang mountains and their tectonothermal overprinting. *Acta Petrol. Sinica.* **2003**, *19*, 131–140, (In Chinese with English Abstract).
29. Wang, Y.J.; Fan, W.M.; Zhang, Y.H. Geochemical, $^{40}Ar/^{39}Ar$ geochronological and Sr–Nd isotopic constraints on the origin of Paleoproterozoic mafic dikes from the southern Taihang Mountains and implications for the ca. 1800 Ma event of the North China Craton. *Precambr. Res.* **2004**, *135*, 55–77. [CrossRef]
30. Wang, Y.J.; Fan, W.M.; Zhang, Y. Structural evolution and ja:math dating of the Zanhuang metamorphic domain in the North China Craton: Constraints on Paleoproterozoic tectonothermal overprinting. *Precambr. Res.* **2003**, *122*, 159–182. [CrossRef]
31. Xiao, L.L.; Wang, G.D. Zircon U-Pb dating of metabasic rocks in the Zanhuang metamorphic complex and its geological significance. *Acta Petrol. Mineral.* **2011**, *3*, 781–794, (In Chinese with English Abstract).
32. Xiao, L.L.; Wu, C.M.; Zhao, G.C. Metamorphic P–T paths of the Zanhuang amphibolites and metapelites: Constraints on the tectonic evolution of the Paleoproterozoic Trans-North China Orogen. *Int. J. Earth Sci.* **2011**, *100*, 717–739. [CrossRef]
33. Trap, P.; Faure, M.; Lin, W. The Luliang Pluton: A key area for the understanding of the Palaeoproterozoic Trans-North China Belt, North China Craton. *Geol. Soc. Lond. Spec. Publ.* **2009**, *323*, 99–125. [CrossRef]

34. Trap, P.; Faure, M.; Lin, W. The Zanhuang Pluton, the second and eastern suture zone of the Paleoproterozoic Trans-North China Orogen. *Precambr. Res.* **2009**, *172*, 80–98. [CrossRef]
35. Yang, C.H.; Du, L.L.; Ren, L.D. *Early Precambrian Stratigraphic Division and Magamtic Evolution in the North Chian Craton*; Science Press: Beijing, China, 2015; pp. 1–277. (In Chinese)
36. Wang, J.P.; Kusky, T.M.; Wang, L.; Wang, S.J.; Deng, H.; Fu, J.M.; Fu, D. Petrogenesis and geochemistry of circa 2.5 Ga granitoids in the Zanhuang Massif: Implications for magmatic source and Neoarchean metamorphism of the North China Craton. *Lithos* **2017**, *268–271*, 149–162. [CrossRef]
37. Xiao, L.L.; Lu, J.S.; Wang, G.D. Geochemistry, metamorphic evolution and its tectonic implications of amphibolites in the southwest area of the Zanhuang complex. *Acta Petrol. Sin.* **2012**, *28*, 2807–2818.
38. Xiao, L.L.; Liu, F.L.; Chen, Y. Metamorphic P-T-t paths of the Zanhuang metamorphic complex: Implications for the Paleoproterozoic evolution of the Trans-North China Orogen. *Precambr. Res.* **2014**, *255*, 216–235. [CrossRef]
39. Liu, C.H.; Zhao, G.C.; Liu, F.L. Zircons U-Pb and Lu-Hf isotopic and whole-rock geochemical constraints on the Gantaohe Group in the Zanhuang Complex: Implications for the tectonic evolution of the Trans-North China Orogen. *Lithos* **2012**, *146*, 80–92. [CrossRef]
40. Xie, H.Q.; Liu, D.Y.; Yin, X.Y. Formation age and tectonic environment of the Gantaohe Group, North China Craton: Geology, geochemistry, SHRIMP zircon geochronology and Hf-Nd isotopic systematics. *Sci. Bull.* **2012**, *57*, 4735–4745. [CrossRef]
41. Black, L.P.; Kamo, S.L.; Allen, C.M.; Aleinikoff, J.N.; Davis, D.W.; Russell, J.; Korsch, R.J.; Chris Foudoulis, C. TEMORA 1: A new zircon standard for Phanerozoic U–Pb geochronology. *Chem. Geol.* **2003**, *200*, 155–170. [CrossRef]
42. Jackson, S.E.; Pearson, N.J.; Griffin, W.L.; Belousova, E.A. The application of laser ablation-inductively coupled plasma-mass spectrometry to in situ U–Pb zircon geochronology. *Chem. Geol.* **2004**, *211*, 47–69. [CrossRef]
43. Ludwig, K.R. *User's Manual for Isoplot/Ex rev. 2.49*; Special publication 1; Berkeley Geochronology Centre: Berkeley, CA, USA, 2003; Volume 56.
44. Andersen, T. Correction of common lead in U-Pb analyses that do not report ^{204}Pb. *Chem. Geol.* **2002**, *192*, 59–79. [CrossRef]
45. Li, H.K.; Geng, J.Z.; Hao, S. Research of determination of U-Pb isotopic age of zircon by laser ablation multi collector plasma mass spectrometer (LA-MC-ICPMS). *Acta Mineral. Sinica.* **2009**, *29*, 600–601. (In Chinese)
46. Collins, W.J.; Beams, S.D.; White, A.J.R.; Chappell, B.W. Nature and origin of A-type granites with particular reference to southeastern Australia. *Contrib. Mineral. Petrol.* **1982**, *80*, 189–200. [CrossRef]
47. Whalen, J.B.; Currie, K.L.; Chappell, B.W. A-type granites: Geochemical characteristics, discrimination and petrogenesis. *Contrib. Mineral. Petrol.* **1987**, *95*, 407–419. [CrossRef]
48. Eby, G.N. The A-type granitoids: A review of their occurrence and chemical characteristics and speculations on their petrogenesis. *Lithos* **1990**, *26*, 115–134. [CrossRef]
49. Liu, C.S.; Chen, X.M.; Chen, P.R. Subdivision, discrimination criteria and genesis for A-type rock suites. *Geol. J. China Univ.* **2003**, *9*, 573–591, (In Chinese with English Abstract).
50. Zhang, Q.; Wang, Y.; Li, C.D. Granite classification on the basis of Yb and Sr contents and its implication. *Acta Petrol. Sin.* **2006**, *22*, 2249–2269, (In Chinese with English Abstract).
51. King, P.L.; White, A.J.R.; Chappell, B.W. Characterization and origin of aluminous A-type granites from the Lachlan Fold Belt, Southeastern Australia. *J. Petrol.* **1997**, *38*, 371–391. [CrossRef]
52. Watson, E.B.; Harrison, T.M. Zircon saturation revisited: Temperature and composition effects in a variety of crustal magma types. *Earth Planet. Sci. Lett.* **1983**, *64*, 295–304. [CrossRef]
53. Bonin, B. A-type granites and related rocks: Evolution of a concept, problems and prospects. *Lithos* **2007**, *97*, 1–29. [CrossRef]
54. Clemens, J.D.; Holloway, J.R.; White, A.J.R. Origin of an A-type granite: Experimental constraints. *Am. Mineral.* **1986**, *71*, 317–324.
55. King, P.L.; Chappell, B.W.; Allen, C.M.; White, A.J.R. Are A-type granites the high-temperature felsic granites? Evidence from fractionated granites of the Wangrah Suite. *Austral. J. Earth Sci.* **2001**, *48*, 501–514. [CrossRef]
56. Miller, C.F.; Mcdowell, S.M.; Mapes, R.W. Hot and cold granites? Implications of zircon saturation temperatures and preservation of inheritance. *Geology* **2003**, *31*, 529–532. [CrossRef]
57. Zhao, G.C.; Wilde, S.A.; Sun, M. Shrimp U-Pb zircon geochronology of the Huai'an Complex: Constraints on late Archean to paleoproterozoic magmatic and metamorphic events in the Trans-North China Orogen. *Am. J. Sci.* **2008**, *308*, 270–303. [CrossRef]
58. Sun, D.Y.; Wu, F.Y.; Gao, S. Confirmation of two episodes of A-type granite emplacement during Late Triassic and Early Jurassic in the Central Jilin Province, and their constraints on the structural pattern of eastern Jilin-Heilongjiang area, China. *Earth Sci. Front.* **2005**, *12*, 263–275, (In Chinese with English abstract).
59. Pearce, J.A.; Harris, N.B.W.; Tindle, A.G. Trace Element Discrimination Diagrams for the Tectonic Interpretation of Granitic Rocks. *J. Petrol.* **1984**, *25*, 956–983. [CrossRef]
60. Auwera, J.V.; Bogaerts, M.; Liégeois, J.P.; Demaiffec, D.; Wilmarta, E.; Olivier Bollea, O.; Duchesnea, J.C. Derivation of the 1.0–0.9 Ga ferro-potassic A-type granitoids of southern Norway by extreme differentiation from basic magmas. *Precambr. Res.* **2003**, *124*, 107–148. [CrossRef]
61. Frost, C.; Frost, B.R. Reduced rapakivi-type granites: The tholeiite connection. *Geology* **1997**, *25*, 647. [CrossRef]
62. Litvinovsky, B.A.; Jahn, B.M.; Zanvilevich, A.N. Petrogenesis of syenite–granite suites from the Bryansky Complex (Transbaikalia, Russia): Implications for the origin of A-type granitoid magmas. *Chem. Geol.* **2002**, *189*, 105–133. [CrossRef]

63. Mushkin, A.; Navon, O.; Halicz, L. The Petrogenesis of A-type Magmas from the Amram Pluton, Southern Israel. *J. Petrol.* **2003**, *44*, 815–832. [CrossRef]
64. Namur, O.; Charlier, B.; Toplis, M.J. Differentiation of Tholeiitic Basalt to A-Type Granite in the Sept Iles Layered Intrusion, Canada. *J. Petrol.* **2011**, *52*, 487–539. [CrossRef]
65. Turner, S.P.; Foden, J.D.; Morrison, R.S. Derivation of some A-type magmas by fractionation of basaltic magma: An example from the Padthaway Ridge, South Australia. *Lithos* **1992**, *28*, 151–179. [CrossRef]
66. Bédard, J. Enclaves from the A-type granite of the Mégantic Complex, White Mountain Magma Series: Clues to granite magmagenesis. *J. Geophy. Res. Atmosph.* **1990**, *95*, 17797–17819. [CrossRef]
67. Kerr, A.; Fryer, B.J. Nd isotope evidence for crust-mantle interaction in the generation of A-type granitoid suites in Labrador, Canada. *Chem. Geol.* **1993**, *104*, 39–60. [CrossRef]
68. Mingram, B.; Trumbull, R.B.; Littman, S. A petrogenetic study of anorogenic felsic magmatism in the Cretaceous Paresis ring complex, Namibia: Evidence for mixing of crust and mantle-derived components. *Lithos* **2000**, *54*, 1–22, 68. [CrossRef]
69. Creaser, R.A.; Price, R.C.; Wormald, R.J. A-type granites revisited Assessment of a residual-source model. *Geology* **1991**, *19*, 163–166. [CrossRef]
70. Anderson, J.L. Proterozoic anorogenic granite plutonism of North America. *Memoir Geol. Soc. Am.* **1983**, *161*, 133–154.
71. Dall'Agnol, R.; Scaillet, B.; Pichavant, M. An Experimental Study of a Lower Proterozoic A-type Granite from the Eastern Amazonian Craton, Brazil. *J. Petrol.* **1999**, *40*, 1673–1698. [CrossRef]
72. Yang, J.H.; Wu, F.Y.; Chung, S.L.; Wilde, S.A.; Zhou, M.F. A hybrid origin for the Qianshan A-type granite, Northeast China: Geochemical and Sr-Nd-Hf isotopic evidence. *Lithos* **2006**, *89*, 89–106. [CrossRef]
73. Skjerlie, K.P.; Johnston, A.D. Vapor-absent melting at 10 kbar of a biotite- and amphibole-bearing tonalitic gneiss: Implications for the generation of A-type granites. *Geology* **1992**, *20*, 263–266. [CrossRef]
74. Eby, G.N. Chemical subdivision of the A-type granitoids:Petrogenetic and tectonic implications. *Geology* **1992**, *20*, 641. [CrossRef]
75. Hong, D.W.; Wang, S.G.; Han, B.F. Post-orogenic alkaline granites from China and comparisons with anorogenic alkaline granites elsewhere. *J. Asian Earth Sci.* **1996**, *13*, 13–27.
76. Zhao, X.F.; Zhou, M.F.; Li, J.W. Association of Neoproterozoic A- and I-type granites in South China: Implications for generation of A-type granites in a subduction-related environment. *Bull. Mineral. Petrol. Geochem.* **2008**, *27*, 1–15. [CrossRef]
77. Lu, S.N.; Zhao, G.C.; Wang, H.C. Precambrian metamorphic basement and sedimentary cover of the North China Craton: A review. *Precambr. Res.* **2008**, *160*, 77–93. [CrossRef]
78. Wu, M.L.; Zhao, G.C.; Sun, M. Petrology and P—T path of the Yishui mafic granulites: Implications for tectonothermal evolution of the Western Shandong Complex in the Eastern Block of the North China Craton. *Precambr. Res.* **2012**, *222–223*, 312–324. [CrossRef]
79. Zhao, G.C.; Guo, J.H. Precambrian geology of China: Preface. *Precambr. Res.* **2012**, *222–223*, 1–12. [CrossRef]
80. Zhao, G.C.; Cawood, P.A.; Li, S.Z. Amalgamation of the North China Craton: Key issues and discussion. *Precambr. Res.* **2012**, *222–223*, 55–76. [CrossRef]
81. Deng, H.; Kusky, T.M.; Polat, A.; Wang, L.; Wang, J.P.; Wang, S.J. Geochemistry of Neoarchean mafic volcanic rocks and late mafic dikes in the Zanhuang Complex, Central Orogenic Belt, North China Craton: Implications for geodynamic setting. *Lithos* **2013**, *175*, 193–212. [CrossRef]
82. Huang, X.L.; Niu, Y.L.; Xu, Y.G.; Yang, Q.J.; Zhong, J.W. Geochemistry of TTG and TTG-like gneisses from Lushan-Taihua complex in the southern North China Craton: Implications for late Archean crustal accretion. *Precambr. Res.* **2010**, *182*, 43–56. [CrossRef]
83. Kröner, A.; Cui, W.Y.; Wang, S.Q.; Wang, C.Q.; Nemchin, A.A. Single zircon ages from high-grade rocks of the Jianping Complex, Liaoning Province, NE China. *J. Asian Earth Sci.* **1998**, *16*, 519–532. [CrossRef]
84. Liu, D.Y.; Shen, Q.H.; Zhang, Z.Q. Archean crustal evolution in China: U-Pb geochronology of the Qianxi Complex. *Precambr. Res.* **1990**, *48*, 223–244. [CrossRef]
85. Liu, D.Y.; Page, R.W.; Compston, W. U-Pb zircon geochronology of late Archaean metamorphic rocks in the Taihangshan—Wutaishan area, North China. *Precambr. Res.* **1985**, *27*, 85–109. [CrossRef]
86. Nutman, A.P.; Wan, Y.S.; Du, L.L. Multistage late Neoarchaean crustal evolution of the North China Craton, eastern Hebei. *Precambr. Res.* **2011**, *189*, 43–65. [CrossRef]
87. Peng, T.P.; Wilde, S.A.; Fan, W.M. Late Neoarchean potassic high Ba–Sr granites in the Taishan granite–greenstone terrane: Petrogenesis and implications for continental crustal evolution. *Chem. Geol.* **2013**, *344*, 23–41.
88. Wan, Y.S.; Liu, D.Y.; Wang, S.J. Juvenile magmatism and crustal recycling at the end of the Neoarchean in Western Shandong Province, North China Craton: Evidence from SHRIMP zircon dating. *Am. J. Sci.* **2011**, *310*, 1503–1552. [CrossRef]
89. Wan, Y.S.; Liu, D.Y.; Wang, S.Y. Early Precambrian Crustal Evolution in the Dengfeng Area, Henan Province (eastern China): Constraints from Geochemistry and SHRIMP U-Pb Zircon Dating. *Acta Geol. Sin.* **2009**, *83*, 982–999.
90. Wan, Y.S.; Dong, C.Y.; Liu, D.Y. Zircon ages and geochemistry of late Neoarchean syenogranites in the North China Craton: A review. *Precambr. Res.* **2012**, *222*, 265–289. [CrossRef]
91. Wang, J.P.; Kusky, T.M.; Polat, A. A late Archean tectonic mélange in the Central Orogenic Belt, North China Craton. *Tectonophysics* **2013**, *608*, 929–946. [CrossRef]

92. Wilde, S.A.; Cawood, P.; Wang, K.Y. The relationship and timing of granitoid evolution with respect to felsic volcanism in the Wutai Complex, North China Craton. In *Proceddings of the 30th International Geological Congress, Beijing, China, 4–14 August 1997*; VSP Internatinal Science Publishers: Amsterdam, The Netherlands, 1997; Volume 17, pp. 75–87.
93. Wilde, S.A.; Cawood, P.A.; Wang, K.Y. Granitoid evolution in the Late Archean Wutai Complex, North China Craton. *J. Asian Earth Sci.* **2005**, *24*, 597–613. [CrossRef]
94. Zhang, H.F.; Zhai, M.G.; Santosh, M. Geochronology and petrogenesis of Neoarchean potassic meta-granites from Huai'an Complex: Implications for the evolution of the North China Craton. *Gondwana Res.* **2011**, *20*, 82–105. [CrossRef]
95. Zhou, Y.Y.; Zhao, T.P.; Wang, C.Y. Geochronology and geochemistry of 2.5 to 2.4 Ga granitic plutons from the southern margin of the North China Craton: Implications for a tectonic transition from arc to post-collisional setting. *Gondwana Res.* **2011**, *20*, 171–183. [CrossRef]
96. Du, L.L.; Yang, C.H.; Wang, W.; Ren, L.d.; Wan, Y.S.; Wu, J.S.; Zhao, L.; Song, H.X.; Geng, Y.S.; Hou, K.J. Paleoproterozoic rifting of the North China Craton: Geochemical and zircon Hf isotopic evidence from the 2137 Ma Huangjinshan A-type granite porphyry in the Wutai area. *J. Asian Earth Sci.* **2013**, *72*, 190–202. [CrossRef]
97. Du, L.L.; Yang, C.H.; Wyman, D.A.; Nutman, A.P.; Zenglong Lu, Z.L.; Song, H.X.; Hangqiang Xie, H.Q.; Wan, Y.S.; Zhao, L.; Geng, Y.S.; et al. 2090–2070Ma A-type granitoids in Zanhuang Complex: Further evidence on a Paleoproterozoic rift-related tectonic regime in the Trans-North China Orogen. *Lithos* **2016**, *254–255*, 18–35. [CrossRef]
98. Du, L.L.; Yang, C.H.; Wyman, D.A.; Nutman, A.P.; Zenglong Lu, Z.L.; Song, H.X.; Zhao, L.; Geng, Y.S.; Ren, L.D. Age and depositional setting of the Paleoproterozoic Gantaohe Group in Zanhuang Complex: Constraints from zircon U-Pb ages and Hf isotopes of sandstones and dacite. *Precambr. Res.* **2016**, *286*, 59–100. [CrossRef]
99. Geng, Y.S.; Du, L.L.; Ren, L.D. Growth and reworking of the early Precambrian continental crust in the North China Craton: Constraints from zircon Hf isotopes. *Gondwana Res.* **2012**, *21*, 517–529. [CrossRef]
100. Wang, J.P.; Kusky, T.M.; Wang, L. Petrogenesis and geochemistry of circa 2.5 Ga granitoids in the Zanhuang Pluton: Implications for magmatic source and Neoarchean metamorphism of the North China Craton. *Lithos* **2016**, 268–271.
101. Xiao, L.L.; Liu, F.L.; Liu, J.H. Geochemistry and its tectonic implications of the Zuoquan-Zanhuang complex. *Acta Petrol. Sin.* **2013**, *29*, 533–550.
102. Pehrsson, S.J.; Berman, R.G.; Rainbird, R. Two Neoarchean supercontinents revisited: The case for a Rae family of cratons. *Precambr. Res.* **2013**, *232*, 27–43. [CrossRef]